PAPER

Check for updates

Morphology, structural, thermal and rheological properties of wheat starch–palmitic acid complexes prepared during steam cooking

Shaoxia Shi, Yaoyao Dong, Qi Li, Tingting Liu and Xiuzhu Yu [ID] *

This work aimed to determine the changes in the morphology, complexation degree, the structural, thermal, and rheological properties of starch–fatty acid complexes during steam cooking. In this study, wheat starch with certain water and palmitic acid contents were steamed for 0.5, 1, 1.5, 2, and 2.5 h. The complexing index (CI) first decreased and then progressively increased with the prolonging of steam cooking time. The decrease in CI was associated with the decomposition of the complex layer formed on the granule surface at 0.5 h of steam cooking. The interaction between wheat starch and palmitic acid led to the change of starch crystal type. Prolonging treatment time promoted thermal stability and structural order degree. The type I and IIa complexes reached saturation and fatty acids in the interstitial space between helices increased with excessive treatment times. Rheological behavior analysis showed that the viscoelasticity and deformation degree of samples decreased and increased, respectively, with increasing steam cooking time. Results showed that the thermostability and order degree of the complex layer were lower than those of samples with long treatment times and complexing was effective during steam cooking.

1. Introduction

In steam cooking, food is cooked using steam from continuous boiling water. Steam cooking, an approach for thermal food preparation, can be traced back to ancient times. It is often performed with a food steamer, which is typically a circular container made of metal or wood and bamboo. Steamed food is kept separate from boiling water by placing it on a grate but comes into direct contact with hot steam and is different from boiled food.[1] The boiling point of water is exactly the highest temperature of the cooked food under normal pressure. Steaming is a healthy method of cooking and is widely enjoyed around the world.[2,3] Steam-cooked products are not only delicious, but they also preserve most of their nutrients, flavor, color, and texture. As a healthy cooking technique, steaming can be used for many kinds of foods. In China, common steamed staple foods, such as steamed bread, steamed twisted rolls, and steamed stuffed buns, are mainly made of flour. Wheat starch accounts for approximately 75% of the dry weight of flour, and the final quality of food products is affected by the pasting, gelatinization, and retrogradation properties of wheat starch.[4,5] Lipids are essential nutrients needed by the human body. They are widely used in food processing to enhance the flavor and taste of food because of their excellent

characteristics, such as crispness, brittleness, and thermal stability. However, food components can interact with each other during processing. During processing, the disruption of starch granule structure results in the dissociation of double helices and the leaching of amylose. These phenomena contribute to the formation of starch–lipid complexes through interactions between lipids and leached amylose. Amylose is a linear glucose polymer and can form left-handed single helices with internal hydrophobic cavities through a conformational change that can result in the formation of inclusion complexes with suitable ligands, such as iodine, fatty acid, and dimethyl sulfoxide.[6,7] In addition, the external branch structures of amylopectin can also form helices.[8] However, amylopectin–lipid complexes are at low amounts, which are difficult to detect given their short branch lengths, low polymerization degree, and large steric hindrance caused by their branched structure. At present, many kinds of methods for inducing starch–lipid complex formation have been found. Using steam jet cooking, Fanta *et al.*[9] prepared nanoparticles with diameters from 63 to 375 nm of amylose–oleic acid inclusion complexes and found that the nanoparticles were comprised of V_6 amylose complexes. Panyoo and Emmambux[10] reported that extrusion cooking of maize starch with certain screw configuration, screw speed, and stearic acid addition significantly decrease the gel texture and first peak viscosity of the maize starch extrudate. Similarly, high-pressure homogenized starch–fatty acid complexes also showed non-gelling properties.[11] In addition to the methods of inducing complex formation by mechanical

College of Food Science and Engineering, Northwest A&F University, 22 Xinong Road Yangling, 712100, Shaanxi, P. R. China. E-mail: xiuzhuyu@nwafu.edu.cn; Fax: +86-29-87092486; Tel: +86-29-87092308

force, there are some others such as deep-frying[12] and heat–moisture treatment.[13] For steam cooking, one of the most important factors is the duration of cooking. Several studies have shown that the starch–lipid complexes formation is related to cooking time.[12,14] Nevertheless, there is a lack of research on the formation and properties of complexes during long-term steam cooking process.

In the present study, the wheat starch–palmitic acid complexes were prepared by steam cooking. Changes in the morphology, complexing index (CI), structural, thermal, and rheological properties of complexes with steam cooking time were investigated using scanning electron microscopy (SEM), iodine blue method, X-ray powder diffraction (XRD), differential scanning calorimetry (DSC), and rheometry. The relationship between the formation and characteristics of the complexes under cooking conditions was clarified to provide theoretical guidance for the production of healthy and nutritious starch-based steamed food.

2. Materials and methods

2.1 Materials and reagents

Wheat starch (moisture 10.1%, lipid 0.25% and amylose content 25.5%) was purchased from Jiangsu Kanghuan Industry and Trade Co., Ltd. (Jiangsu Province, China). Palmitic acid was obtained from Aladdin Chemistry Company (Shanghai, China). All other chemical reagents were of analytical grade.

2.2 Preparation of wheat starch–palmitic acid complexes

The steam cooking experiments were carried out using a steamer (Midea Group Co., Ltd., Guangdong Province, China). The steamer is approximately cylindrical in shape, which is composed of lid, body, and grate. Generally, the function of the grate is to support the food, so that the water vapor and heat can be better absorbed by the samples. The material of steamer is 304 stainless steel and its geometrical features are as follows: thickness, 0.8 mm; the body height, 16 cm; the lid height, 6 cm; and inner diameter, 24.5 cm. The amount of water added in the steamer was 1.8 L, and it was heated in an electric ceramic stove with a heating power of 500 W. During water boiling, the steam temperature at the sample location was 102.5 °C and the pressure is about 95 300 Pa. In the process, the heat energy prepared by the electric ceramic stove is mainly transferred to the liquid water in the steamer by heat conduction. Liquid water vaporizes into steam, which contacts the sample and transfers heat to it.

The prepared wheat starch solution (80%, w/w) was placed in glass Petri dishes (10 cm in diameter), covered with plastic film to prevent water loss, and then equilibrated for 12 h. Palmitic acid (30%, w/w) was evenly added to the wheat starch solution. The complex was steam cooked with the steamer for 0.5, 1, 1.5, 2, and 2.5 h; dried at room temperature; ground; and passed through a 60-mesh sieve. For the removal of free fatty acid residues, all samples were washed with ethanol and centrifuged (3800 × g, 10 min) to collect samples. Native wheat starch prepared with the same procedure without adding palmitic acid and steam cooking was used as a control. All samples were dried in air of room temperature to volatilize residual ethanol and sealed in zip-lock bags at room temperature for further analysis.

2.3 SEM

A small amount of powder sample was evenly distributed on the double-sided conductive paste of the sample stage. Excess powder sample was removed under high-pressure air, and the sample stage was sprayed using a sputter coater (Q150TS, Quorum). The external structure of samples was observed with a scanning electron microscope (Nova Nano SEM 450, FEI) in low vacuum mode and viewed under 1500× magnification. All samples were examined using an accelerating voltage of 5 kV.

2.4 Complex content

The complex content was determined through a modified iodine blue method as follows:[4] the powder sample (0.1 g) was weighed accurately into a 50 mL centrifuge tube and then mixed with 5 mL of distilled water. The suspension was stirred in a boiling water-bath for 35 min to fully gelatinize starch. After cooling to room temperature, 25 mL of distilled water was added to the above gelatinized starch sample. The sample was vortexed for 2 min and centrifuged for 15 min at 3800 × g. Then, 400 μL of the supernatant was mixed with 8.6 mL of distilled water and then with 1 mL of iodine solution (2.0% KI and 1.3% I_2 in distilled water). The tube was inverted several times, and absorbance was measured at 690 nm. Native wheat starch treated in the same manner was used as a reference. The complex content was calculated using the following equation:

$$CI\ (\%) = 100(A_w - A_{w-p})/A_w$$

where A_w is the absorbance of the wheat starch solution and A_{w-p} is the absorbance of the wheat starch–palmitic acid complex solution.

2.5 XRD

An X-ray diffractometer (Rigaku Miniflex, Japan) with a λ value of 1.5406 Å and operating at an acceleration potential of 40 kV with 30 mA current and copper target was used to obtain the wide-angle XRD spectra of all samples. The scanning range was 4–40° (2θ) at a speed of 5° min^{-1} (2θ) and with a step size of 0.02° (2θ). The experiment was performed at room temperature.

2.6 DSC

Thermal transition properties were measured using a Q2000 differential scanning calorimeter (TA Instruments, New Castle, DE, USA). The instrument was periodically calibrated with indium. First, different samples were weighed (approximately 3 mg) into an aluminum pan. Deionized water (9 μL) was added to the samples. The pans were hermetically sealed and allowed to equilibrate under room temperature for more than 12 h. Finally, the samples were analyzed by first being equilibrated at 30 °C for 2 min and then being heated to 150 °C at a rate of 10 °C min^{-1} under nitrogen atmosphere. An empty and sealed pan was used as a reference. The peak temperature (T_p) and

enthalpy change (ΔH) were obtained and analyzed using TA Universal Analysis 2000 software.

2.7 Rheological properties

The rheological behavior of samples was quantified by using a rheometer (DHR-1, TA Instrument, USA). Sample suspensions of 6% (w/v) were stirred in a boiling water-bath for 0.5 h and transferred to a rheometer plate with a parallel plate system (40 mm in diameter) after cooling to room temperature for rheological tests. The gap size was set at 1.0 mm. The sample edge was covered with a thin layer of methyl silicone oil to minimize evaporation loss. Frequency sweep tests were performed over the range of 0.1–200 rad s^{-1}. The strain amplitude for the frequency sweep measurements was selected as 10%, which is within the linear viscoelastic region. Creep tests were performed with a stress level of 0.8 Pa. All test procedures were conducted at 25 °C.

2.8 Statistical analysis

All experiments were repeated three times, and the results were reported as the mean values and standard deviations. Only one measurement was performed for rheological properties. Significant differences between means were determined through the LSD test at a significance level of 0.05 using Minitab 18.1 (Minitab Inc., PA, USA) software.

3. Results and discussion

3.1 Morphology

The external structures of native starch and wheat starch–palmitic acid complexes were analyzed using SEM (Fig. 1). SEM micrographs revealed that native starch (Fig. 1a) contained large (10–35 μm) A-type and small (1–10 μm) B-type granules which were round to oval in shape.[15] However, as seen from the micrographs of wheat starch–palmitic acid complexes obtained by steam cooking for 0.5 h to 2.5 h (Fig. 1b–f), the granules have been destroyed to varying degrees. Notably, the morphology of the complexes varied greatly with the duration of steam cooking. When starches were cooked for a short duration with limited amounts of water, the water molecules absorbed by the granules were bound tightly and were not freely mobile. Thus, the granules were not completely damaged, and intact starch

granules were retained during short steam cooking times (Fig. 1b). In addition, the presence of irregularly shaped fragments on the surfaces of swollen wheat starch granules indicate amylose leaching,[16] which might facilitate the formation of a complex layer on the granule surface. For the sample of 0.5 h, palmitic acid did not diffuse in starch granules but coat around it to form the complex layer. However, the gradual disappearance of granules with the prolongation of steam cooking time suggested that the additional steam absorbed by the granules was converted into water, which could move within the granules during continuous steam cooking to further disrupt starch crystallites. Lamellae appeared during this process. Folded nuclei lamellae are attributed to intra- or even inter-hydrogen bonding between carboxyl groups and hydroxyl groups,[17] confirming that the structure of the complexes is semicrystalline. Moreover, few holes were found on the surfaces of crystalline fragments obtained through 2.5 h of steam cooking (Fig. 1f).

3.2 Complexing index

CI represents the percentage of complexation between starches and lipids.[18] The effect of treatment time on CI during steam cooking is shown in Table 1. The CIs of the wheat starch–palmitic acid complexes first decreased and then increased progressively from 0.5 h to 2.5 h. Notably, a turning point was observed at 1 h, and the minimum CI of the wheat starch–palmitic acid complexes could reach 65.27%, which reflected effective complexation through steam cooking. Furthermore, as shown in the above SEM micrograph, the granule structures of complexes were intact before 1 h of steam cooking but were destroyed after 1 h of steam cooking. Therefore, the decrement in CI value in the former phase may have resulted from the decomposition of complex polymorphs.[12] The CI value gradually tended to increase as the steam cooking time increased in the latter phase. Given that the disintegrated starch granules released amylose under excessive treatment time, additional complexes were formed.

3.3 Crystalline structure

The diffraction diagrams of samples obtained at different steam cooking times are presented in Fig. 2. As illustrated in Fig. 2, native starch presented typical A-type XRD patterns with peaks at 15.1°, 16.9°, 18°, and 23°. The characteristic peaks at 12.9°
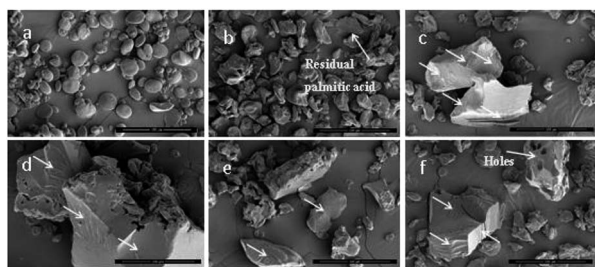

Fig. 1 SEM micrographs of native starch (a), wheat starch–palmitic acid complexes at steam cooking times of 0.5 (b), 1 (c), 1.5 (d), 2 (e), and 2.5 h (f). Unmarked arrows indicate lamellae (magnification 1500×).

Table 1 CI of native starch and wheat starch–palmitic acid complexes during steam cooking^{a,b}

Samples	CI (%)
Native starch	ND
Steam cooking 0.5 h	73.36 ± 1.04^{a}
Steam cooking 1 h	65.27 ± 1.47^{b}
Steam cooking 1.5 h	69.36 ± 1.56^{ab}
Steam cooking 2 h	73.01 ± 0.87^{a}
Steam cooking 2.5 h	73.53 ± 2.08^{a}

^{a} Values are means ± SD. Different letters in a column indicate significant differences ($p < 0.05$). ^{b} ND, not detected.
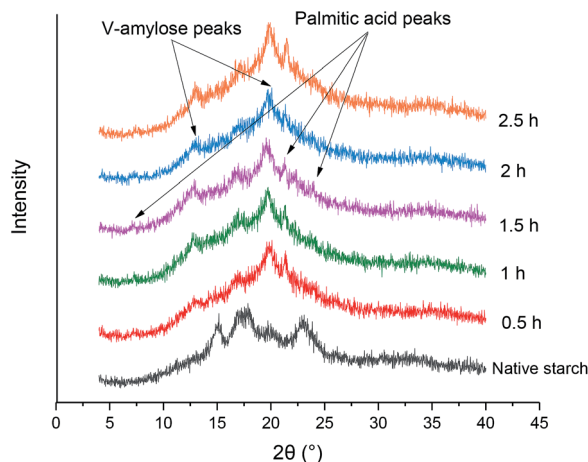
Fig. 2 XRD spectra of native starch and wheat starch–palmitic acid complexes during steam cooking.

and 20° that corresponded to V-type structures were found in the patterns of wheat starch–palmitic acid complexes formed through steam cooking. The X-ray diffractogram of the complexes displayed a combination of A- and V-crystalline structures with peaks at 12.9°, 16.9°, and 20°. Among these structures, the A-crystalline structure at the peak of 16.9° indicated undamaged starch and retrograded starch. Moreover, the diffractograms of wheat starch–palmitic acid complexes revealed three extra peaks at 7.2°, 21.3°, and 24° attributed to the presence of fatty acid crystals.[19]

All the complexes except 0.5 h had no significant change in the V-type peak intensity. It indicated that prolonging treatment time had little effect on the crystalline structure of the complexes after the particle structure was destroyed. The peak intensity of 0.5 h at 12.9° was significantly weaker than that of other complexes. It could be due to the lower order of the complex layer formed in 0.5 h. The peak of fatty acid crystal at 21.3° formed in 2.5 h showed strong diffraction signals that reflected the increase in palmitic acid in the interstitial space between helices (Fig. 2) and implied connections with the holes observed from SEM results (Fig. 1f).

3.4 Thermal properties

The thermal properties of native starch and wheat starch–palmitic acid complexes during steam cooking as measured by

DSC are summarized in Table 2. All the samples appeared as endothermic peaks. As shown in Table 2, the first peak of native starch was attributed to wheat starch gelatinization, and the second was attributed to the dissociation of the complex formed through the interaction of amylose with a small amount of endogenous lipids. Nevertheless, the first peak of the complexes was attributed to the additive effect of free palmitic acid melting and wheat starch gelatinization. The second and third corresponded to the dissociation of types I and IIa starch–lipid complexes, respectively, but no intermediate form was detected. On the basis of previous studies, type I complexes with low order decomposed over the temperature range of 96 °C to 104 °C, whereas semicrystalline type IIa (114 –121 °C) and IIb (121 –125 °C) complexes have higher melting temperatures. The complexing and crystallizing of the type IIa polymorph was slower than type I. During slow isothermal crystallization, the type I complexes can be transformed into type II forms. Annealing of the type IIa complex at above 90 °C also resulted in the formation of IIb polymorphs.[20,21] High melting temperature reflects high thermal stability and structural order. The peak temperature of type I and IIa starch–lipid complexes slightly increased as the steam cooking time increased (Table 2). These findings implied that the thermal stability of starch–lipid complexes was improved by long reaction time.

The enthalpy change (ΔH) of the second and third peak could reflect the amount of the two types of complexes. The total amounts of the two types of complexes were basically in agreement with the trend of the CI values. SEM results revealed that a complex layer was present on the granule surfaces of the sample of 0.5 h. Meanwhile, in the second peak, the thermal stability of the complex layer treated for 0.5 h was lower than that of the complex sample treated for more than 0.5 h. Therefore, the decomposition of the complex layer with low thermal stability after 0.5 h reduced the CI and suggested that the formation of type I complexes depended not only on treatment time, but starch morphology. The ΔH value slightly increased after 1 h, which might be due to more leached amylose from disintegrated starch granules under excessive treatment time. Unlike that of type I complexes, prolonged steam cooking time resulted in a slow increase of small amount of type IIa complexes. This effect indicated that the nucleation rate of type IIa complexes was lower than type I. Additionally, the ΔH of complexes in the first peak should progressively

Table 2 Thermal parameters of native starch and wheat starch–palmitic acid complexes during steam cooking[a,b]

| Samples | Peak I | | Peak II | | Peak III | | Peak II + peak III |
	T_p (°C)	ΔH (J g^{-1})	T_p (°C)	ΔH (J g^{-1})	T_p (°C)	ΔH (J g^{-1})	ΔH (J g^{-1})
Native starch	62.58 ± 0.73[a]	8.21 ± 0.25[a]	97.67 ± 0.58[b]	1.55 ± 0.09[c]	—	—	—
Steam cooking 0.5 h	62.09 ± 0.48[a]	1.83 ± 0.01[cd]	98.17 ± 0.15[b]	4.41 ± 1.12[a]	115.94 ± 0.85[b]	0.34 ± 0.21[c]	4.75 ± 1.36[a]
Steam cooking 1 h	62.49 ± 0.04[a]	2.04 ± 0.13[c]	100.31 ± 0.04[a]	1.96 ± 0.04[c]	115.46 ± 0.98[b]	0.54 ± 0.02[b]	2.50 ± 0.05[b]
Steam cooking 1.5 h	62.19 ± 0.42[a]	1.77 ± 0.03[d]	100.00 ± 0.88[a]	2.74 ± 0.08[b]	117.45 ± 0.35[a]	0.90 ± 0.04[a]	3.64 ± 0.10[ab]
Steam cooking 2 h	61.96 ± 0.17[a]	1.70 ± 0.06[d]	100.12 ± 0.56[a]	3.01 ± 0.00[b]	117.19 ± 0.00[a]	0.96 ± 0.04[a]	3.97 ± 0.00[ab]
Steam cooking 2.5 h	61.91 ± 0.38[a]	2.75 ± 0.01[b]	100.90 ± 0.95[a]	3.22 ± 0.01[b]	118.37 ± 0.35[a]	1.07 ± 0.13[a]	4.29 ± 0.01[a]

[a] T_p, peak temperature; ΔH, enthalpy change. [b] Values are means ± SD. Different letters in a column indicate significant differences ($p < 0.05$).

decrease with the prolongation of steam cooking time if only wheat starch gelatinization is considered. However, the ΔH value of the sample that was steam cooked for 2.5 h was significantly higher than that of others. This difference could reflect the contribution of palmitic acid in the interstitial space between helices, which is related to the strong diffraction signal of the peak at 21.3° formed in 2.5 h by XRD and the holes observed from SEM results. As a result, the content of type I and IIa complexes was close to saturation after 1.5 h, but excessive treatment time would promote the increase of fatty acids in the interstitial space between helices.

3.5 Rheological properties

3.5.1 Oscillation measurement: frequency sweep. In general, storage modulus (G') indicates that stress energy is temporarily stored during the test but can be recovered afterward. The loss modulus (G'') hints at the fact that the energy that has been used to initiate flow is irreversibly lost having been transformed into shear heat. The ratio of G'' to G' is defined as the loss tangent tan δ (G''/G'). Complex viscosity ($\eta*$) describes the total resistance to dynamic shear.

As shown in Fig. 3a–c, the G', G'', and $\eta*$ of all samples progressively decreased with the prolongation of steam cooking time. This behavior reflected that viscoelasticity decreased under the influence of treatment time. The samples with treatment time more than 1 h (including 1 h) presented that G'' was higher than G', indicating that the complexes formed after the destruction of the particle structure were mainly viscous behavior. For native starch, boiling in a water-bath for 0.5 h during pretreatment resulted in starch pasting. During the

subsequent cooling process, available amylose molecules interacted closely to form junction zones by hydrogen bonds. This led to the formation of a stable gel through molecular entanglement.

However, the junction zones formed in the starch–lipid complex were limited, which caused complexes to align more easily in the direction of shear and the density of hydrogen bonds decreased.[22] The negligible effect of the complex layer formed in 0.5 h on the viscoelastic response of the sample paste might be due to the decomposition of the complex layer during gelatinization in the pretreatment. Therefore, the curve trend of the sample that was processed for 0.5 h was similar to that of native starch. Simultaneously, G' and G'' showed frequency dependence, indicating that the stress energy temporarily stored and the shear heat (i.e., energy lost) increased with the increasing angular frequency (ω).

The viscoelastic behavior of samples can be reflected by the tan δ value. Tan δ < 1 indicates predominantly elastic behavior, which is reflected by viscoelastic solids, and tan δ > 1 indicates mainly viscous behavior, which is reflected by viscoelastic liquid. The tan δ values of the wheat starch–palmitic acid complexes formed through 1–2.5 h of steam cooking were considerably higher than those of native starch and the complexes formed in 0.5 h. This result indicated that viscous properties were greatly promoted by the presence of complexes rather than by the decomposition of the complex layer during pretreatment in a boiling water-bath (Fig. 3d).

3.5.2 Step (transient) measurement: creep. The creep test is also used to differentiate between the viscous and the elastic responses of a test specimen. The creep compliance (J) is a time-related term, and high J can facilitate the deformation of
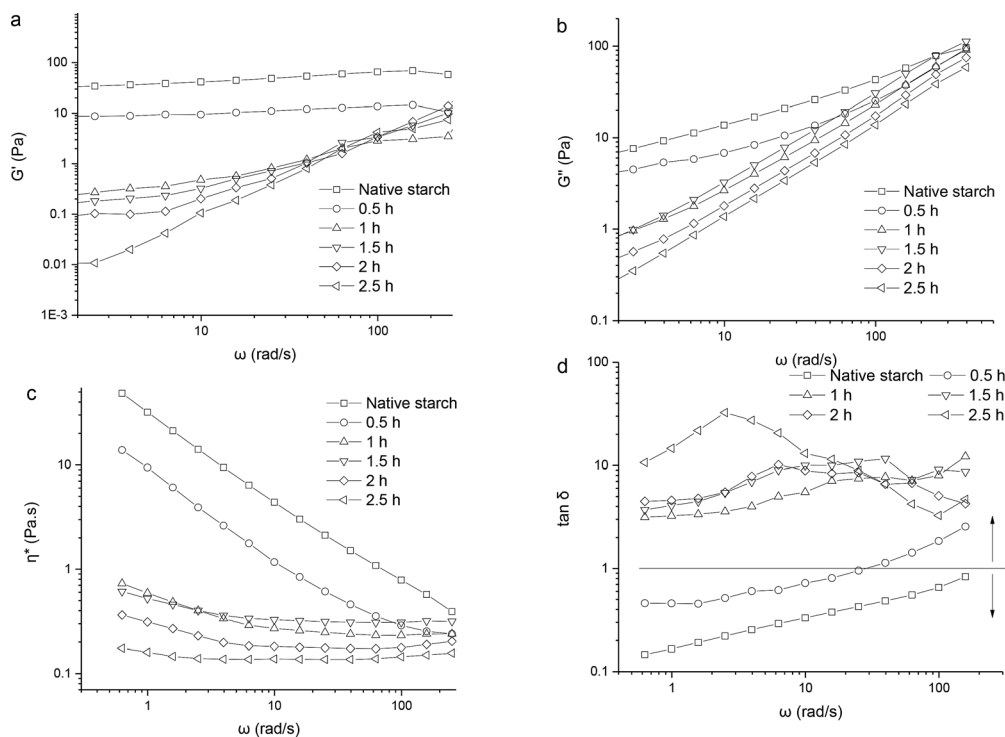

Fig. 3 Effect of treatment time on the G' (a), G'' (b), tan δ (c), and $\eta*$ (d) of native starch and wheat starch–palmitic acid complexes.
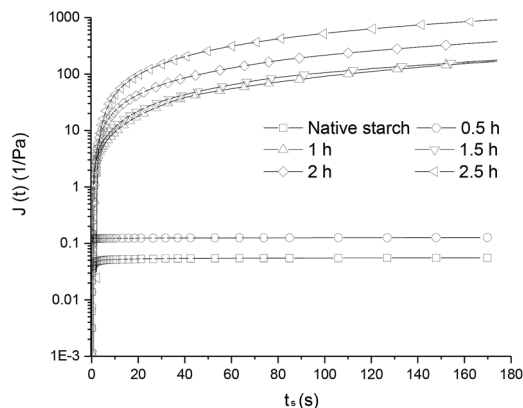
Fig. 4 Effect of treatment time on the J of native starch and wheat starch–palmitic acid complexes.

a sample under a given stress. Elastic components can be stretched to their mechanical limits under constant stress in the early phase of the creep test. Then, they will float within the matrix mass, and the sample will exhibit viscous flow.[23]

The J curves gradually increased with the prolongation of steam cooking time. This behavior revealed that the matrix structure became weaker and more deformable, suggesting that the elastic components were present in high proportions. This result was consistent with the trend for CI value after steam cooking for 1 h (Fig. 4). The high degree of deformation may be attributed to the reduction in hydrogen bond density. Frequency sweep and creep test showed that the trends exhibited by the sample of 0.5 h and that shown by native starch were similar. The reasons might be that the complex layer formed in 0.5 h not only enhanced the hydrophobicity of the granules but hindered the entry of palmitic acid molecules into starch particle. These effects inhibited the further formation of the complex and kept the particle structure to a certain degree.

4. Conclusions

The effective formation of wheat starch–palmitic acid complexes during steam cooking was confirmed, and treatment time could considerably affect the extent of complex formation. The thermal stability and order degree of the complex layer on granule surface were lower than those of the complexes formed under longer treatment time. The interaction between wheat starch and palmitic acid changed starch crystal type. The thermostability and structural order degree of the complexes were improved with the prolongation of steam cooking time. Furthermore, excessive treatment time would lead the type I and IIa complexes to reach saturation but promote the increase of fatty acids in the interstitial space between helices. The reduction in viscoelasticity was mainly affected by the reduction in hydrogen bond density in the sample paste. The potential differences in stability between the complex layer on the granule surface and complex formed by steam cooking and their practical process research should be further investigated.

Abbreviations

CI	Complexing index
SEM	Scanning electron microscopy
XRD	X-ray powder diffraction
DSC	Differential scanning calorimetry
T_p	Peak temperature
ΔH	Enthalpy change
G'	Storage modulus
G''	Loss modulus
η^*	Complex viscosity
ω	Angular frequency
J	Creep compliance

Conflicts of interest

Shaoxia Shi, Yaoyao Dong, Qi Li, Tingting Liu and Xiuzhu Yu declare that they have no conflict of interest.

Acknowledgements

References

1 D. J. Horrobin, K. A. Landman and L. Ryder, *Ind. Eng. Chem. Res.*, 2003, **42**, 4109–4122.
2 S. Caparrotta, E. Masi, G. Atzori, I. Diamanti, E. Azzarello, S. Mancuso and C. Pandolfi, *Sci. Hortic.*, 2019, **256**, 108540.
3 M. Modzelewska-Kapitula, R. Pietrzak-Fiecko, K. Tkacz, A. Draszanowska and A. Wiek, *Meat Sci.*, 2019, **157**, 107877.
4 M. C. Tang and L. Copeland, *Carbohydr. Polym.*, 2007, **67**, 80–85.
5 J. D. Wilson, D. B. Bechtel, T. C. Todd and P. A. Seib, *Cereal Chem.*, 2006, **83**, 259–268.
6 J. A. Putseys, L. Lamberts and J. A. Delcour, *J. Cereal Sci.*, 2010, **51**, 238–247.
7 C. K. Reddy, S. M. Choi, D. J. Lee and S. T. Lim, *Food Chem.*, 2018, **244**, 136–142.
8 S. Wongprayoon, T. Tran, O. Gibert, E. Dubreucq, K. Piyachomkwan and K. Sriroth, *Starch - Stärke*, 2018, **70**, 1700351.
9 G. F. Fanta, J. A. Kenar and F. C. Felker, *Ind. Crops Prod.*, 2015, **74**, 36–44.
10 A. E. Panyoo and M. N. Emmambux, *Starch - Stärke*, 2019, **71**, 1800149.
11 S. A. Oyeyinka, S. Singh, Y. Ma and E. O. Amonsou, *RSC Adv.*, 2016, **6**, 80174–80180.
12 Y. Yang, L. Wang, Y. Li, H. F. Qian, H. Zhang, G. C. Wu and X. G. Qi, *Food Chem.*, 2019, **283**, 287–293.
13 X. Chen, X. He, X. Fu, B. Zhang and Q. Huang, *Int. J. Biol. Macromol.*, 2017, **98**, 557–564.

14 J. Alvarez-Ramirez, E. J. Vernon-Carter, H. Carrillo-Navas and M. Meraz, *LWT–Food Sci. Technol.*, 2018, **91**, 203–212.

15 E. Chiotelli and M. Le Meste, *Cereal Chem.*, 2002, **79**, 286–293.

16 B. Chen, X. Jia, S. Miao, S. Zeng, Z. Guo, Y. Zhang and B. Zheng, *Food Chem.*, 2018, **252**, 115–125.

17 A. Marinopoulou, E. Papastergiadis, S. N. Raphaelides and M. G. Kontominas, *Food Hydrocolloids*, 2016, **58**, 224–234.

18 L. Wang, W. Wang, Y. Wang, G. Xiong, X. Mei, W. Wu, A. Ding, X. Li, Y. Qiao and L. Liao, *Int. J. Food Prop.*, 2018, **21**, 2121–2134.

19 A. Marinopoulou, E. Papastergiadis and S. N. Raphaelides, *Starch - Stärke*, 2019, **71**, 1800100.

20 J. Karkalas, S. Ma, W. R. Morrison and R. A. Pethrick, *Carbohydr. Res.*, 1995, **268**, 233–247.

21 S. J. Wang, C. Chao, J. J. Cai, B. Niu, L. Copeland and S. Wang, *Compr. Rev. Food Sci. Food Saf.*, 2020, **19**, 1056–1079.

22 J. Agyei-Amponsah, L. Macakova, H. L. DeKock and M. N. Emmambux, *Starch - Stärke*, 2019, **71**, 1800340.

23 D. D. Milasinovic, *Int. J. Solids Struct.*, 2004, **41**, 4599–4634.